

## Separation of Kinetic and Potential Electron Emission Arising from Slow Multicharged Ion-Surface Interactions

I. G. Hughes, J. Burgdörfer, L. Folkerts, C. C. Havener, S. H. Overbury, M. T. Robinson, D. M. Zehner, P. A. Zeijlmans van Emmichoven,\* and F. W. Meyer

*Oak Ridge National Laboratory, Oak Ridge, Tennessee 37831-6372*

(Received 1 March 1993)

Characteristic variations in the total electron yield  $\gamma$  as a function of crystal azimuthal orientation are reported for slow  $N^{2+}$ ,  $N^{5+}$ , and  $N^{6+}$  ions incident on a Au(011) single crystal. These variations allow the direct separation of kinetic and potential electron emission, and allow, for the first time, an analysis of the neutralization dynamics of multicharged ions interacting with a metal surface, above the kinetic emission threshold. Electron emission resulting from below-surface Auger transitions is shown to be the dominant potential emission mechanism.

PACS numbers: 79.20.Rf, 34.90.+q

Traditionally it has been useful to define electron emission in ion-surface interactions as kinetic electron emission (KEE) or potential electron emission (PEE), depending on whether the ejected electrons are liberated by the conversion of kinetic or potential energy of the incident projectile. While KEE can occur only after the incident ion has impacted the target surface, for multicharged ion projectiles PEE can already begin at relatively large distances above the surface with stepwise neutralization into high-lying Rydberg levels of the incident ion, leading to the formation of a so-called "hollow" atom [1]. The deexcitation of this "hollow" atom above the target surface may proceed via a cascade of interatomic and projectile-based intra-atomic Auger processes. Electrons may also be emitted above the surface when high-lying projectile Rydberg states are promoted to the continuum with decreasing distance as a result of the interaction of the captured electrons with the projectile image potential, or by the screening effect of more tightly bound electrons [1,2]. Recently it has been shown [3,4] that the completion of the complex cascade of Auger processes responsible for multicharged ion neutralization above the target surface requires time scales of the order of  $10^{-12}$  to  $10^{-13}$  s. For shorter above-surface interaction times, it is likely that the incident projectiles will still be in a multiexcited state when they reach and interact with the surface. Sudden screening of the projectile core charge by the high density of valence band electrons within the target will result in any remaining Rydberg electrons becoming unbound and "peeled" from the projectile at the moment of surface penetration [1]. Subsequent electron capture in the bulk will take place into lower-lying  $n$  states followed by rapid inner shell intra-atomic Auger transitions [3]. While promotion, "peel-off" electron emission, and below-surface PEE are all possible at higher projectile velocities where the above-surface cascade is incomplete, the increasing contribution from KEE makes the experimental determination of the relative contributions of these neutralization processes more difficult.

We present in this Letter measurements as well as a modeling analysis of the total secondary electron yields,

$\gamma$ , for  $N^{2+}$ ,  $N^{5+}$ , and  $N^{6+}$  ions incident on a Au(011) single crystal, in the velocity range 0.25–0.55 a.u. Characteristic variations in  $\gamma$  are reported as a function of the incident azimuthal angle. Variations of the ion-induced electron emission with target azimuth angle have been reported previously [5], as a means of orienting monocrystalline targets. The present azimuthal variations allow us to unambiguously separate the contribution of KEE to the total electron yield, and hence to investigate, for the first time, the mechanisms responsible for PEE in the energy region above the kinetic emission threshold. From our analysis we conclude that the major contribution to PE in this energy region arises from secondary cascade processes within the target bulk, rather than from above-surface neutralization processes. This conclusion provides a new perspective from which to view electron emission in multicharged ion-surface interactions.

We have carried out a range of measurements of the total electron yield for  $N^{2+}$ ,  $N^{5+}$ , and  $N^{6+}$  ions incident on a clean Au(011) single crystal surface. The details of our apparatus and technique have been given elsewhere [3]. Briefly, a beam of multicharged ions, extracted from the Oak Ridge National Laboratory electron cyclotron resonance (ORNL-ECR) ion source, was directed onto a Au(011) single crystal mounted on a manipulator. The crystal surface was prepared by cycles of sputter cleaning and annealing, and the surface cleanliness was verified using Auger electron spectroscopy. To obtain the total electron yield  $\gamma$ , the current to the crystal was measured both with and without a positive bias voltage applied to hold the secondary electrons. A target bias of +300 V, giving over 95% suppression of the secondary electron emission, was employed under normal incidence conditions to obtain the incident ion flux. The measurements were carried out at pressures of typically  $10^{-8}$  Pa.

In Fig. 1(a), we present our measurements of the total electron yield as a function of the crystal azimuthal angle for 30 keV  $N^{2+}$ ,  $N^{5+}$ , and  $N^{6+}$  ions at  $20^\circ$  incidence. The total electron yield can be seen to exhibit characteristic azimuthal variations. The amplitude of these

variations in Fig. 1(a) is seen to be independent of the incident ion charge state. Similar measurements of the azimuthal variations in the total electron yield for 80 keV  $N^{5+}$  and  $N^{6+}$  are shown in Fig. 1(b) for the same incidence conditions. It can be seen that the amplitude of the variations has increased with incident ion kinetic energy.

Recent semiempirical theories [6] of low-energy KEE are based on the observation that the total electron yield and the mean inelastic (or electronic) stopping power of the projectile follow the same dependence on the incident ion kinetic energy. The degree of electronic stopping in

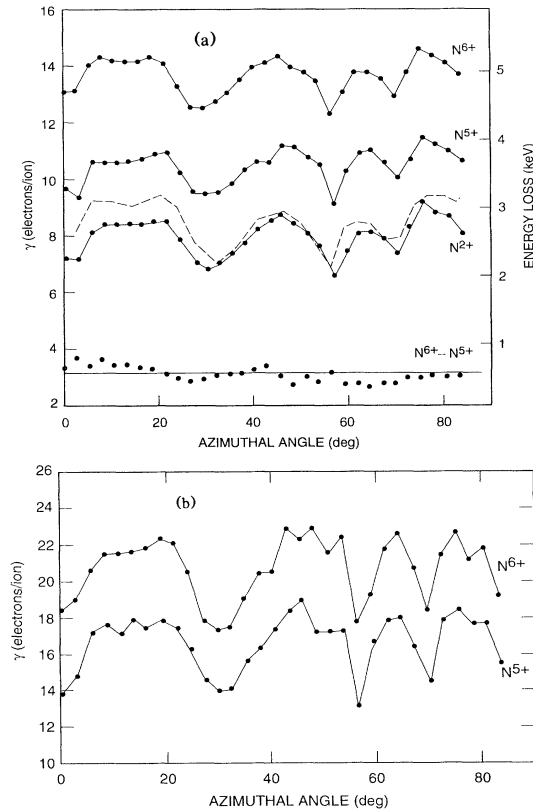


FIG. 1. (a) Total electron yield  $\gamma$  as a function of crystal azimuthal angle  $\phi$  for 30 keV  $N^{2+}$ ,  $N^{5+}$ , and  $N^{6+}$  ions incident at  $20^\circ$  on Au(011). The absolute yields for  $N^{5+}$  and  $N^{6+}$  have been normalized to correspond to the straight line fits of Fig. 2 at the appropriate azimuthal angle ( $6^\circ$  to the [100] direction). The average local inelastic energy loss calculated using the MARLOWE trajectory code for 5000 30 keV N ions at  $20^\circ$  on traversing a 40 Å slab is shown as a dashed line.  $0^\circ$  corresponds to the [100] direction. The difference in yield between  $N^{6+}$  and  $N^{5+}$  shown in (a) is seen to be essentially azimuthally invariant. The straight line drawn through the difference points represents the average over all azimuths, equal to  $3.1 \pm 0.4$ . (b) Total electron yield  $\gamma$  as a function of crystal azimuthal angle  $\phi$  for 80 keV  $N^{5+}$  and  $N^{6+}$  ions incident at  $20^\circ$  on Au(011). The absolute yields for  $N^{5+}$  and  $N^{6+}$  have been normalized to correspond to the straight line fits of Fig. 2 at the appropriate azimuthal angle.  $0^\circ$  corresponds to the [100] direction.

turn depends on the electron density sampled along the projectile ion trajectory in the target bulk. Since the electron density is maximum at lattice sites, and since for a single crystal the mean distance of closest approach in a collision between an incident ion and a target surface atom will vary with crystal orientation, variations in the electronic stopping and hence the total electron yield are expected as a function of crystal azimuthal angle.

We have used the MARLOWE Monte Carlo simulation code [7] to calculate the energy loss of the incident projectiles on traversing a target of finite thickness. In the MARLOWE code, the trajectory of each projectile ion is followed collision by collision as it interacts with the atoms of the target. Each collision is assumed to consist of an elastic and inelastic part. The elastic part is described by classical scattering theory using the Moliere approximation to the Thomas-Fermi potential with the screening length proposed by Firsov [8]. The inelastic part consists of a local inelastic energy loss  $Q$ , corresponding to electron excitation or ionization, which occurs at the apsis of the encounter and is given by

$$Q(s, E) = \frac{0.045KE^{1/2}}{\pi a_{12}^2} \exp[-0.3R(s, E)/a_{12}], \quad (1)$$

where  $s$  is the impact parameter in the collision,  $E$  is the kinetic energy of the projectile,  $a_{12}$  is the screening length in the Moliere potential,  $R$  is the apsis of the trajectory, and  $K$  is a parameter whose value is determined using the theory of Lindhard, Scharff, and Schiott [9] at high energies where  $R(s, E) \approx s$ . This form of the local inelastic energy loss was chosen to reflect approximately the electron density around the target atoms. The electronic stopping associated with Eq. (1) is

$$S_e = 2\pi \int_0^{s_c} s Q(s, E) ds, \quad (2)$$

where  $s_c$  is the maximum value of the impact parameter determined by the lattice dimensions of the target.

Figure 1(a) shows the local inelastic energy loss, calculated using MARLOWE, on traversing a slab of thickness 40 Å averaged over 5000 incident ion trajectories for 30 keV N atoms incident at  $20^\circ$  on a Au(001) single crystal as a function of crystal azimuthal orientation. The thickness of the target layer was chosen to be of the same order as the inelastic mean free path for low-energy electrons, but the results presented here do not depend critically on the slab thickness chosen. It can be seen that the local inelastic energy loss exhibits azimuthal variations very similar to those observed experimentally in the total electron yield. We therefore attribute the azimuthally varying component of the total electron emission to KEE. The nonlocal inelastic energy loss, representing collective excitation loss mechanisms, was also calculated, but is expected to make only a minor contribution to the secondary electron yield due to the low conversion efficiency of plasmon oscillations to free electrons in the present velocity regime.

We can obtain the contribution to the total electron yield due to the initial ion charge state by subtracting the spectra for  $N^{6+}$  and  $N^{5+}$  incident ions. This contribution, shown in Fig. 1(a) for 30 keV incidence energy, is found to be essentially azimuthally invariant, and, furthermore, to have the same magnitude for both 30 and 80 keV incident ions. We have checked the velocity independence of this charge-state-dependent component by measuring the total electron yield as a function of incident ion velocity for  $N^{5+}$  and  $N^{6+}$  ions under the same incidence conditions. As can be seen in Fig. 2, the additional emission for  $N^{6+}$  as compared to  $N^{5+}$  is independent of projectile velocity within our present velocity range. The invariance of this component with incident ion velocity indicates that it is not due to enhanced KEE in the topmost layers of the target due to the initial ion charge. On this basis, we are able to separate the KEE from the total electron yield and to attribute the charge-state-dependent but velocity-independent component to PEE. A similar velocity-independent component has recently been deduced by Kurz *et al.* [10], using a technique based on the analysis of electron emission statistics [11] at much lower incident ion energies, where KEE is a minor component of the total electron yield.

The separation of the PEE component from the KEE allows us for the first time to investigate the neutralization of multicharged ions in a velocity region where KEE is the majority contributor to the total electron yield. As pointed out above, the following mechanisms may contribute to the PEE component: (i) above-surface PEE (i.e., cascade), (ii) above-surface electron promotion to the continuum, (iii) peel off due to sudden screening on surface impact, and (iv) subsurface PEE. To obtain a quantitative estimate of the contribution of both the above-surface Auger cascade and the promotion to the continuum to the total electron yield, we have used the

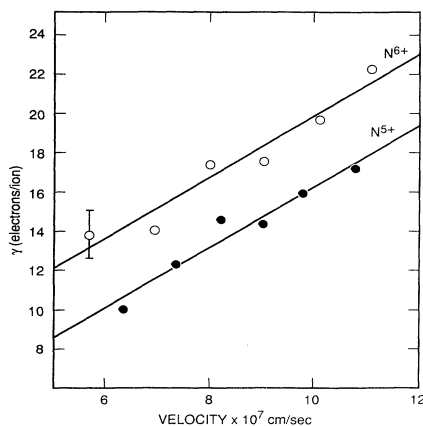


FIG. 2. Total electron yield  $\gamma$  as a function of incident ion velocity for  $N^{5+}$  and  $N^{6+}$  ions incident at  $20^\circ$  on Au(011) for a fixed crystal azimuth. Solid lines are least-squares fits to data points.

classical over-the-barrier model. The model simulations, the details of which have been presented elsewhere [1], give an estimate for emission into  $4\pi$  sr of  $\sim 1.2$  electrons per ion for the above surface PEE, and  $\sim 0.17$  electron per ion for promotion to the continuum, at the lower limit of the velocity range of the present experiment. The corresponding contributions at the upper velocity limit are  $\sim 0.6$  and  $\sim 0.04$  electron per ion, respectively. These estimates represent an upper limit to the expected contributions, and are likely to significantly overestimate the actual electron yield. In addition, it can be seen that the contributions from both above-surface PEE and promotion to the continuum exhibit a significant dependence on the incident ion velocity. This is in contrast to the observed velocity independence of the PEE component. It would appear, therefore, that electrons arising from above-surface PEE and above-surface promotion to the continuum comprise only a minor part of the charge-state-dependent emission in the present energy range.

In order to determine the possible contribution from peel-off electrons, we have used the over-the-barrier model to estimate the populations of those projectile levels which become unbound at the moment of surface impact. It is expected that for incident  $N^{6+}$ , levels with  $n \leq 3$  remain bound below the surface [3]. We have, therefore, summed the population for levels  $n \geq 4$ , which for  $N^{6+}$  is found to be  $\sim 7.5$  electrons and remains essentially constant within our present energy range. For incident  $N^{5+}$ , the same analysis yields a summed population for  $n \geq 4$  of  $\sim 6.3$  electrons, which again remains constant in the present energy range. The formation of a negative ion in front of the surface deduced from the above level populations has been noted previously [12]. The observed velocity behavior of the PEE component in the present case may therefore be consistent with the peel-off mechanism. However, since the outer level populations for  $N^{6+}$  increase only by one electron compared to  $N^{5+}$ , the peel-off mechanism is not able to account for the large PEE yield increase of  $\sim 3.5 \pm 0.4$  e/ion observed for  $N^{6+}$  in comparison to  $N^{5+}$ . (This error is calculated from the standard deviation of the mean for the straight line fits in Fig. 2.) It would appear, therefore, that while peel-off electrons may contribute, they are not responsible for the major part of PEE. A similar conclusion has recently been reached by Kurz *et al.* [10]. One implication of this analysis is that only a minor fraction of the peel-off electrons are backscattered from the surface. We are unable to offer an *a priori* estimate of the contribution of peel-off electrons to the observed electron yield, due to the unknown fate of these electrons. Whether such electrons are promoted to the continuum or are captured into the metal conduction band is not known. The term "peel-off" simply refers to the Rydberg electrons becoming unbound from the projectile.

By this process of elimination we are left with the conclusion that below-surface PEE is the major contribution to the velocity-independent yield in the present case. We

can consider the below-surface PEE to be composed of two distinct contributions, which we shall call direct PEE and indirect PEE. Direct PEE consists of Auger electrons which escape from the surface without undergoing inelastic collisions within the bulk. Such electrons will be detected at the corresponding Auger transition energies. Indirect PEE consists of those Auger electrons which do undergo inelastic collisions, together with any secondary electrons which they generate within the bulk and which are able to escape into vacuum.

Since only levels with  $n \leq 3$  are expected to be bound within the bulk [3], direct PEE is comprised essentially of *KLL* and *LMM* Auger transitions. This projectile-based electron emission would be expected to decrease with increasing projectile perpendicular velocity, as the ion penetrates further into the target material and the electron escape probability decreases. This expected trend in the velocity dependence of *KLL* and *LMM* Auger electrons has been previously reported [13] for 24 keV  $N^{6+}$  ions incident on Cu(100). In addition, from our earlier analysis [3], the number of *KLL* and *LMM* electrons observed at their original transition energies appears insufficient to account for the magnitude of the PEE component.

In contrast to direct PEE, the total number of low-energy secondary electrons produced by indirect PEE is expected to be much less projectile velocity dependent due to their significantly longer inelastic mean free paths and resulting higher probabilities for escape from larger depths. In addition, a 3–4 *e*/ion increase of indirect PEE for  $N^{6+}$ , compared to  $N^{5+}$ , is to be expected due to an increase in secondary processes involving the high-energy *KLL* Auger electron emitted below the surface. Such a yield difference has been previously observed [13] for  $N^{5+}$  and  $N^{6+}$  ions incident on Cu(100). Also, in contrast to the strong incidence angle dependence found for the projectile *K* Auger electron emission, only a very weak dependence was found for the  $N^{6+}$ - $N^{5+}$  yield difference, consistent with the above picture for indirect subsurface PEE. The experimental evidence is therefore consistent with the conclusion that the major contribution to PEE above the KE threshold arises from below-surface PEE, due to secondary cascade processes initiated by Auger transitions occurring within the target bulk. We would like to point out that by inclusion of subsurface indirect PEE processes, it is not necessary for us to invoke the “ultimate” autoionization and Auger neutralization processes proposed by Kurz *et al.* [10] to explain the velocity-independent components of their measured electron yields. Consequently, a reassessment of present models for the filling of electronic states prior to the inner-shell vacancy-related fast Auger electron emission, as suggested by Kurz, would not appear to be required in the projectile energy range considered in the present experiments.

In summary, we present in this paper measurements of

the total electron yields for  $N^{2+}$ ,  $N^{5+}$ , and  $N^{6+}$  ions incident on a Au(011) single crystal in the velocity range 0.25–0.55 a.u. The total electron yield is seen to consist of two distinct components, an azimuthally varying velocity-dependent component, and an azimuthally invariant velocity-independent component. Using the MARLOWE trajectory code we are able to unambiguously attribute these components to KEE and PEE, respectively, and to investigate, for the first time, the mechanisms responsible for PEE in the energy region above the kinetic emission threshold. From our analysis we conclude that the major contribution to PE in this energy region arises from “indirect PEE” due to secondary cascade processes within the target bulk.

This work was supported by the Office of Basic Energy Sciences and by the Division of Applied Plasma Physics of the U.S. Department of Energy, under Contract No. DE-AC05-84OR21400 with Martin Marietta Energy Systems, Inc. We gratefully acknowledge J. Hale and G. Ownby for their skilled technical assistance, and H. P. Winter for his insightful comments on our findings.

---

\*Present address: Buys Ballot Laboratorium Utrecht, University of Utrecht, NL-3584 CC Utrecht, The Netherlands.

- [1] J. Burgdörfer, P. Lerner, and F. W. Meyer, *Phys. Rev. A* **44**, 5674 (1991).
- [2] S. Y. Ovchinnikov and J. Macek, in Proceedings of the Sixth International Conference on the Physics of Highly Charged Ions, Kansas, September 1992 (to be published).
- [3] F. W. Meyer, S. H. Overbury, C. C. Havener, P. A. Zeijlmans van Emmichoven, and D. M. Zehner, *Phys. Rev. Lett.* **67**, 723 (1991); F. W. Meyer, S. H. Overbury, C. C. Havener, P. A. Zeijlmans van Emmichoven, J. Burgdörfer, and D. M. Zehner, *Phys. Rev. A* **44**, 7214 (1991).
- [4] J. Das and R. Morgenstern, *Phys. Rev. A* **47**, R755 (1993).
- [5] H. H. W. Feijen, L. K. Verhey, A. L. Boers, and E. P. Th. M. Suurmeijer, *J. Phys. E* **6**, 1174 (1973).
- [6] R. A. Baragiola, E. V. Alonso, and A. Oliva Florio, *Phys. Rev. B* **19**, 121 (1979).
- [7] M. T. Robinson, *Phys. Rev. B* **27**, 5347 (1983); O. S. Oen and M. T. Robinson, *Nucl. Instrum. Methods* **132**, 647 (1976).
- [8] O. B. Firsov, *Zh. Eksp. Teor. Fiz.* **33**, 696 (1958) [*Sov. Phys. JETP* **6**, 534 (1958)].
- [9] J. Lindhard, M. Scharff, and H. E. Schiott, *K. Dan. Vidensk. Selsk., Mat. Fys. Medd.* **33**, 14 (1963).
- [10] H. Kurz, K. Töglhofer, H. P. Winter, F. Aumayr, and R. Mann, *Phys. Rev. Lett.* **69**, 1140 (1992).
- [11] G. Lakits, A. Arnau, and H. P. Winter, *Phys. Rev. B* **42**, 15 (1990).
- [12] J. Burgdörfer and F. W. Meyer, *Phys. Rev. A* **47**, R20 (1993).
- [13] P. A. Zeijlmans van Emmichoven, C. C. Havener, and F. W. Meyer, *Phys. Rev. A* **43**, 1405 (1991).